Proceedings of CHT-17
ICHMT International Symposium on Advances in Computational Heat Transfer

May 28-June 1, 2017, Napoli, Italy

CHT-17-195

COMPUTATIONAL INSIGHTS INTO SUSTAINABILITY OF OSCILLATIONS IN A SINGLE BRANCH PULSATING HEAT PIPE

U. Bhardwaj*,§ and S.P. Das*
*Department of Mechanical Engineering, Indian Institute of Technology Madras, Chennai, India
§Correspondence author. Email: u.bhardwaj88@yahoo.in

ABSTRACT Pulsating heat pipes (PHPs) are the two-phase flow based thermal management devices prominently researched and developed over a last few years. Their applications for the systems consisting of dense electronic circuitry have been considerably explored. Several installations have been found to be running successfully. But, still there are several industrial thermal management domains practically untouched by the pulsating heat pipes, due to the poor reliability levels of the latter. As the reliability majorly depends upon the tendency of PHP oscillations to sustain or decay, so the authors focused over the sustainability of oscillations as the primary concern rather than the concerns regarding performance level of an operating PHP. So, this paper gives a computational insight about what all determines the likeliness of oscillations to sustain or decay. Focus has been put over some extremities leading to the oscillations which always decay. Limelight has been given to the effect of "operational triad" on the sustainability of oscillations. Operational triad which influences deeply the sustainability of oscillations, has been taken as a combination of the hot and cold section temperatures of PHP, and the fluid reservoir pressure. Various combinations of these three elements of the triad have been explored, to determine what kinds of their combination promote the oscillations to decay and what all kinds of their combination promote the oscillations to sustain. For different extremities within the triad, the mechanism and factors owing to the decay of oscillations have been studied in details. For each case, graphical solutions have been found and PHP functioning has been visualized.

NOMENCLATURE

C_f friction coefficient
d tube diameter (m)
F force (N)
h_{lv} latent heat of vaporization (J/kg)
m mass (kg)
U heat transfer coefficient (W/(K m^2))
v meniscus velocity (m/s)
x meniscus position (m)

Subscripts
a adiabatic section

c	condenser section/condensation
d	dry part of evaporator
e	evaporator section/evaporation
f	liquid film, friction
g	dry vapour/gas (without liquid film)
l	liquid
max	maximum
min	minimum
r	reservoir
sat	at saturation
v	vapour
0	at t = 0

INTRODUCTION

To meet the extensive requirements of thermal management of the circuit card assemblies, satellites, printed circuit boards, microprocessors, avionics, solar collectors, space crafts, any other electronic circuitry, pulsating heat pipes (PHPs) have emerged in the recent past as one of the best solutions technically [Zhang and Faghri, 2008]. Basically, a PHP is a capillary tube of significant length taken either as straight or bent into many turns. In case of a multi-turn PHP, the end-points of the tube may or may not be connected with each other, forming a closed loop or open loop PHP respectively. Generally, a low boiling point and two-phase working fluid is filled into it with some filling ratio, which can be either a single component fluid or a nano fluid. When it is heated over some length at one end, called as “evaporator section” and cooled over some length at another end called as “condenser section”, a train of vapour bubbles and liquid plugs gets formed in the tube. These two sections may be separated by an insulated section known as “adiabatic section”. In a realistic scenario, the evaporator section is nothing but the system being cooled, or some associated subsidiary to the main system being cooled. Once the threshold limits are exceeded, self-sustained oscillations get triggered within the train of vapour bubbles and liquid plugs. These self-sustained oscillations are driven by the evaporation of the working fluid inside the hot section and condensation of the vapour inside the cold section. Thin film dynamics plays a very important role in these oscillations, as showcased experimentally by Rao et al. [2013, 2015]. The heat is thus absorbed from one end and rejected at another end, showcasing an effective transport of heat through a miniature tube. Apart from the latent heat transfer, there is transfer of sensible heat too. This leads to the superheating of vapour inside the evaporator section and sub-cooling of the liquid inside the condenser section. The heat flux requirements emerge out from the applicative considerations. The PHP is designed accordingly. It should be noted that unlike conventional heat pipes [Faghri, 1995], there is no wick structure present in PHPs thus avoiding any counter-current flow between liquid and vapour.

Considerable development has taken place in the research and development of PHPs after the same was invented by Akachi et al. [1996]. But still when it comes to the question of their industrial application, PHPs have been often disregarded. This may be due to inherent complexity in the system owing to the inter-dependence of a large number of variables and parameters associated with their functioning. So owing to the well experienced functioning uncertainties, the reliability level of the PHPs is still questionable in practical scenario. A lot of work has been carried out over the performance analysis/enhancement of well-functioning PHPs in the recent past by Jun and Kim [2016], Wu et al. [2016], Goshayeshi et al. [2016], Shi et al. [2016], Jiansheng, Zhenchuan and Meijun [2014], Kearney [2016], Cui et al. [2016]. Das et al. [2010] studied experimentally the functioning of a single branch PHP, but the focus has been on the operating conditions where the oscillations were sustained. Vadim [2013] has carried out stability analysis for a single branch PHP without adiabatic section, finding the instability threshold symbolically for the same. But now, a need has been felt to go into deep quantitative aspects regarding operational parameters of PHP. It has been found helpful in knowing the qualitative inter-dependence of these parameters in determining the sustainability of oscillations. Moreover for a specific PHP the functioning of which is uncertain in long-run, there is not much point in talking about the performance enhancement. So as of now, authors focused over the serious concerns faced regarding halt of PHP oscillations. Ensuring the sustainability of oscillations has been considered more of primary importance.

So, here a single branch horizontal PHP consisting of an adiabatic section between the evaporator and condenser sections has been considered for analysis. The system has been characterized mathematically by main five and some other subsidiary governing differential equations using Film Evaporation/Condensation (FEC) Model [Das et al., 2010]. A "Rigid-end Flexible-end (REFE) approach" has been devised to take into account the frictional uncertainties and inertia of the liquid plug. The devised methodology keeps on adjusting the length of liquid plug in numerical computations as per the transient conditions during operation. The focus has been put over the three prominent operational parameters, evaporator section temperature, condenser section temperature and the fluid reservoir pressure. The combination of these three parameters has been termed as "operational triad". Analysis has been carried out to sort out the different natures of operational triad which promote the oscillations to decay and sustain respectively. Triad extremities leading to always decaying oscillations have been found out. For each of the cases, the oscillations' decay mechanism has been given a detailed visualization.

MATHEMATICAL MODELING

Model Geometry The model considered here depicts a single branch, straight and horizontal PHP as shown in Fig. 1 with major dimensions in symbolic form. It is basically a capillary tube of uniform internal diameter "d" assumed to be aligned axi-symmetrically along x-axis. To the left, there is the "evaporator section (E)" having length "L_e" and wall temperature "T_e" throughout its length. To the second from right, there is the "condenser section (C)" having length "L_c" and wall temperature "T_c" throughout its length. Separating these two sections, there is an insulated section known as "adiabatic section (A)" with length "L_a".

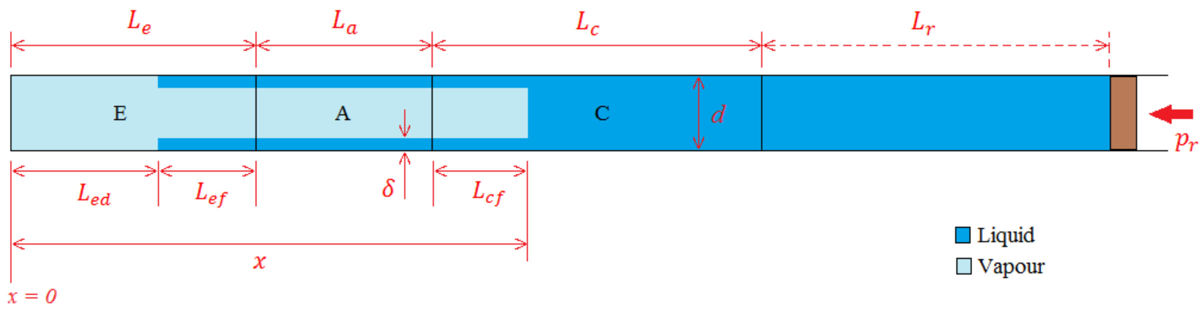

Fig. 1. Schematic of the model for a single branch horizontal PHP

Here, PHP consists of only one vapour bubble and one liquid plug. Instantaneous location of the meniscus has been indicated by "x" measured from the extreme left end of the PHP. During the operation of PHP, there are times when there is a thin film partially covering the evaporator section wall, the instantaneous length of which has been denoted by "L_{ef}". The corresponding dry portion of the evaporator wall has been characterized by its length "L_{ed}". Whenever a part of vapour bubble is lying inside the adiabatic and/or condenser section, their respective wall is always covered by the thin liquid film enclosing the vapour bubble across the contained length of the same. The instantaneous length of the liquid film inside the condenser section has been denoted by "L_{cf}". The thickness of liquid film has been assumed always constant throughout its instantaneous length as "δ". Though it is well expected that the film thickness will vary with the evaporation and condensation processes, it can be noted that it also varies along its length while getting deposited by the moving meniscus owing to the transient velocity of the latter. It is clear from the discussions given by Fairbrother and Stubbs [1935], Bretherton [1961], Aussilous and Quéré [2000], Han and Shikazono [2009].

Under the REFE approach, one end of the PHP which is lying at the evaporator section's outer boundary has been taken as a closed and rigid end. Another end of the PHP which is lying beyond the condenser section's outer boundary, has been provided with a hypothetical and frictionless sliding piston (thus inducing "flexibility"). There has been considered some extra length of fluid extended beyond the condenser section which acts as a fluid reservoir during PHP oscillations. It takes part in oscillations as well. It has been taken in such a way that the piston never enters the condenser action during oscillations. A constant pressure "p_r" has been assumed over the piston which keeps the fluid intact inside PHP. This pressure mimicries the fluid reservoir pressure for a real case scenario. Here onwards it will be referred to as "reservoir pressure" only, which is actually exerted under the combined effect of reservoir's vapour pressure and the hydrostatic pressure due to liquid column there.

During oscillations, the piston also oscillates coupled with the meniscus. Though the piston velocity is always a bit less than that of the meniscus due to incorporation of the thin liquid film. This way, the dynamic length of the liquid plug gets incorporated into the model and the corresponding frictional loss due to sweeping motion of the same along the PHP wall gets accounted in. The variability of the effective liquid plug length has been taken care of by having flexibility and adjustability of the piston's position w.r.t. meniscus's position. This meniscus-piston coupling resulted into better consideration of corresponding dynamic friction.

It can be noted that the vapour bubble is characterized by its pressure "p_v" and temperature "T_v", whereas the liquid plug is characterized by its length $(L_t + L_r - x)$, where $L_t = (L_e + L_a + L_c)$.

Governing Equations: Film Evaporation/Condensation Model Using this model, several equations have been formulated for the model geometry under consideration. Each of them has been explained in this section.

The meniscus displacement and velocity are linked by the equation, $v = \dot{x}$ (1)

Hence, $v > 0$ indicates that meniscus is moving from evaporator section towards condenser section and vice-versa. Dry length of the evaporator section is given by,

$$\dot{L}_{ed} = \begin{cases} v & if \quad L_{ed} \geq x, \ v < 0 \\ \dfrac{\dot{m}_{ef}}{\rho_l \pi d \delta} & otherwise \end{cases} \tag{2}$$

where, $\dot{m}_{ef}$ is the film mass evaporation rate inside the evaporator section as explained within this section. L_{ed} indicates the instantaneous position of the film front from the extreme left end of PHP. Length of the liquid film inside the evaporator and condenser sections at any moment of time is respectively given by equations below.

$$L_{ef} = \begin{cases} x - L_{ed} & if \quad L_{ed} < x \leq L_e \\ 0 & if \quad x \leq L_{ed} \\ L_e - L_{ed} & if \quad x \geq L_e \end{cases} \qquad L_{cf} = \begin{cases} 0 & if \quad x \leq L_e + L_a \\ x - (L_e + L_a) & if \quad L_e + L_a < x \leq L_e + L_a + L_c \\ L_c & otherwise \end{cases}$$

Except for the conditions corresponding to very high T_e and very small T_c, evaporation/condensation from/to the meniscus is respectively negligible as compared to the corresponding quantities related with the thin liquid film. Rate of film mass evaporation and condensation in the evaporator and condenser sections respectively are given by, $\dot{m}_{ef} = U_e \pi d L_{ef}(T_e - T_{satp})/h_{lv}$ and $\dot{m}_{cf} = U_c \pi d L_{cf}(T_c - T_{satp})/h_{lv}$ respectively. Here, T_{satp} is the saturation temperature of working fluid corresponding to the instantaneous pressure p_v of the vapour bubble, as given below [NIST Chemistry Webbook].

$$T_{satp} = \exp\Big(5.059 + 0.039167\log(p_v) + 0.0012452\big(\log(p_v)\big)^2 - (5.3621e-5)\big(\log(p_v)\big)^3 + (7.9644e-6)\big(\log(p_v)\big)^4\Big)$$

where, p_v is in Pa and T_{satp} is in K.

Thus, overall effect of simultaneously going-on evaporation and condensation processes gives the estimate of rate of change of vapour mass inside the vapour bubble, as given by equation (3).

$$\dot{m}_v = \dot{m}_{ef} + \dot{m}_{cf} \tag{3}$$

The energy equation for the vapour bubble is given by equation (4).

$$m_v c_{vv} \dot{T}_v = \dot{m}_v R_v T_v + U_g \pi d L_{ed}(T_e - T_v) - p_v S v \tag{4}$$

Here, the second term on the right hand side indicates the sensible heat transfer between the vapour and the dry wall of the evaporator section whereas the third term is a measure of the work done by/over the vapour bubble during expansion/compression. The momentum equation for the liquid plug can be written as,

$$\frac{d(m_l v)}{dt} = (p_v - p_r)S - F_\sigma - F_f * signum \tag{5}$$

where, $m_l = (L_t + L_r - x)S\rho_l$ is the liquid mass at an instant, $S = (\pi d^2/4)$ is the cross-sectional area of PHP, and $signum = \begin{cases} -1 & if \quad v < 0 \\ 0 & if \quad v = 0 \\ 1 & if \quad v > 0 \end{cases}$

F_f is the single-phase frictional force same as given by Das et al. [2010]. F_σ is the force due to surface tension on the liquid plug given by, $F_\sigma = \sigma\pi(\mathrm{d} - 2\delta)$.

Pressure and mass of the vapour bubble are linked with each other by equation of state (6) assuming the vapour to be behaving like an idea gas as considered by Dobson [2004, 2005], Shafii, Faghri and Zhang [2001].

$$p_v = \frac{m_v R_v T_v}{Sx} \tag{6}$$

Now, for getting the dynamic length of the liquid plug as per REFE approach, we need to formulate the extended length L_r. It is well known [de Gennes, 1985] that the viscous friction prevalent in the vicinity of the junction of the moving meniscus with the film or dry PHP wall can be very large. So the initial value of L_r denoted by "L_{r0}" ($L_{r0} = 5L_t$) has been taken large enough to increase the effective length of the liquid plug. This roughly compensates the deficit in single-phase flow friction compared to much higher two-phase flow friction, thus makes the frictional loss estimation more realistic and reliable. Now, an expression for the initial effective length "L_{i0}" of the liquid plug using the initial meniscus position "x_0" can be written as, $L_{i0} = L_t - x_0 + L_{r0}$. The instantaneous value of L_r is thus given by,

$$L_r = \begin{cases} L_{i0} - (L_t - x) & if \quad x \le L_e \\ L_{i0} - (L_t - x) - \dfrac{4(x - L_e)(d - \delta)\delta}{d^2} & if \quad L_e < x \le L_e + L_a + L_c \\ L_{i0} + (x - L_t) - \dfrac{4(x - L_e)(d - \delta)\delta}{d^2} & otherwise \end{cases} \tag{7}$$

Here, the last term in the second line and third lines correspond to the hypothetical length of liquid plug equivalent to the amount of liquid film present inside the PHP, partially or fully inside the adiabatic/condenser sections depending upon the meniscus location, and fully inside the adiabatic and condenser sections plus a part of extended section depending upon the meniscus location, respectively. The mass of film present inside the evaporator section has been neglected in this context as it would be comparably very thin and short for a considerable fraction of an oscillation. It is to be noted that the film cross sectional area is based on its average diameter $(d - \delta)$.

PARAMETER QUANTIFICATION

For a set of system and operational parameters, differential equations (1) to (5) have been solved in MATLAB using "ode23s" solver which is based on a modified Rosenbrock formula of order 2. The working fluid being implied is "n-pentane". The thermophysical properties of the working fluid have been thus taken as, $R_v = 115.23\ \mathrm{J/(kg\ K)}$, $\rho_L = 626\ \mathrm{kg/m^3}$, $\mu_L = 2.894 \times 10^{-4}$ Pa s, $c_{vv} = 1603.44\ \mathrm{J/(kg\ K)}$, $\sigma = 0.01703\ \mathrm{N/m}$, and $h_{lv} = 357450\ \mathrm{J/kg}$. The thickness of the thin liquid film has been taken as "80 μm" which lies in the range defined by the two values used by Das et al. [2010]. The heat transfer coefficients used are, $U_e = 2000\ \mathrm{W/(m^2K)}$, $U_c = 1500\ \mathrm{W/(m^2K)}$ and $U_g = (1/50)\,U_e$, approximated on the basis of thermal resistance (conduction) offered by the PHP wall and thin liquid film in addition to the thermal resistance offered to the convective heat transfer from/to heating/cooling fluids to/from the PHP at its outer surface. The principal system parameters have been taken as, $d = 2$ mm, $L_e = 200$ mm, $L_a = 100$ mm and $L_c = 300$ mm. Inner diameter of the PHP has been taken lesser than the critical diameter corresponding to the working fluid under consideration which in turn is given by the Bond number [Zhang and Faghri, 2008]. The lengths of the sections have been chosen roughly in the average range depicted by the cited literature. L_c has been taken more than L_e because $U_e > U_c$, and overall heat transfer rate for the two need to be same. Initial conditions used are: $x_0 = 150$ mm, $v_0 = 0$, $\delta_0 = 1$ mm and $T_{v0} \approx 26$ °C. Further in the upcoming sections, temperatures for the evaporator section have been chosen taking care of the safe and practical limits for any general electronic circuitry, while those of the condenser section have been taken to meet the cooling flux requirements for the corresponding length and T_e under consideration.

RESULTS AND DISCUSSION

Operational Triad: Oscillation Sustainability Threshold As already mentioned, the operational triad is composed of three principal operational parameters, viz., evaporator section temperature (T_e), condenser section temperature (T_c) and the fluid reservoir pressure (p_r).

It has been found that at a given condenser temperature and reservoir pressure, there exists a minimum threshold temperature of the evaporator such that oscillations always decay below the threshold. As meniscus starts moving towards the condenser from its extreme position inside the evaporator ($v > 0$), the vapour pressure inside the bubble keeps increasing till it reaches the condenser's inner boundary. This is due to ongoing film evaporation inside the evaporator section with no condensation happening anywhere as demonstrated by Rao et al. [2013]. Thus p_v will be maximum at $x = L_e + L_a$ ($v > 0$) if meniscus reaches there, otherwise somewhere at $L_e < x < L_e + L_a$. Now, the penetration into condenser is determined by the fluid reservoir pressure and is likely to be prevented soon if $p_{v\_max} < p_r$. Some minimum T_e at a given p_r is required to facilitate the meniscus penetrating into the condenser. For a given T_c and p_r, evaporator temperature near to its threshold value may be just able to sustain the oscillations with a very small amplitude. This way it can be sorted out that higher is the reservoir pressure, higher will be the threshold T_e. In fact the threshold T_e has been found to be almost directly proportional to the p_r irrespective of the condenser section temperature, as shown in Fig. 2. Conversely it can be concluded that at a given condenser section temperature, there exists a maximum value of p_r for each T_e such that oscillations will always decay for values of p_r higher than that. Maximum allowable p_r for oscillations to sustain is almost directly proportional to T_e.

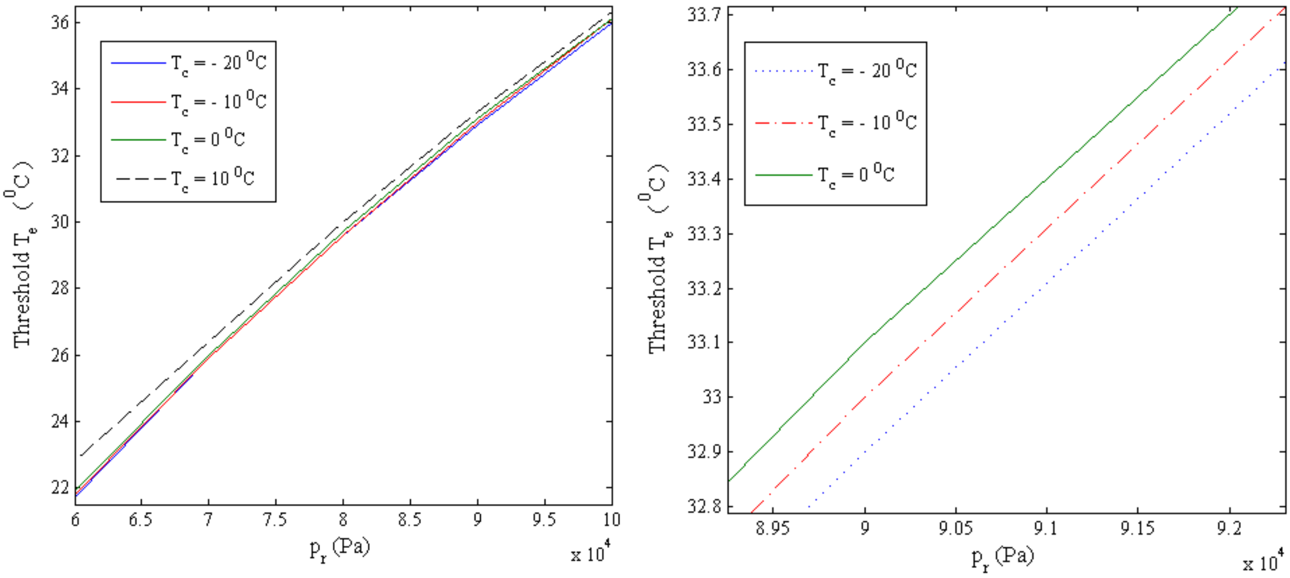

(a) (b)

Fig. 2 (a) and (b) Sustainability threshold w.r.t. operational triad

An important observation from this figure is that the oscillation sustainability is prominently determined by the T_e value alone rather than the difference $(T_e - T_c)$, especially at smaller values of T_c. It means if T_c is small, then the threshold T_e depends majorly on the p_r (in the operational triad) and very weakly on T_c. It is so because the heat absorbed inside the evaporator section which primarily depends on T_e and meniscus penetration inside it (as it determines the length of film deposited there), needs to be equal to the heat rejected to the condenser section which in turn depends upon T_c and meniscus penetration inside it. Also, higher is the T_c, larger is the heat transfer area inside the condenser section required to reject the absorbed heat and vice-versa. Thus more is the penetration of meniscus inside the condenser section and maximum L_{cf}, and vice-versa. Hence the penetration of meniscus inside the condenser section (or x_{max}) is adjusted as per the actual T_c value, p_r being constant. As the vapour pressure reaches a minimum value (p_{v_min}) due to ongoing vapour mass reduction (owing to condensation) and vapour expansion, meniscus stops for a moment at its extreme position somewhere inside the condenser section and then traverses back towards inner condenser boundary. During this whole trip of meniscus through condenser, the condensation that would have happened would be sufficient enough to reject the required amount of heat because of any T_c value which is not so high. This is the reason why the plots for $T_c = -20, -10$ and 0 °C are so close to each other in Fig. 2 (a). The lines are almost coinciding with each other having extremely small gaps in-between as clear from a magnified view (Fig. 2 (b)) of the small portion of Fig. 2 (a). But as T_c is increased beyond a limit at same T_e, condensation happens very slowly and thus p_v decreases prominently due to vapour expansion rather than condensation. Meniscus stops as soon as p_v reaches a minimum value, and then traverses back towards inner condenser boundary. As the meniscus penetration, stoppage and reversal is governed majorly by vapour expansion now, only a fraction of the total absorbed heat can be rejected to the condenser section due to higher T_c till the meniscus enters back into adiabatic section (v < 0). This phenomenon leads the oscillations to decay due to heat and mass accumulation as explained later.

But if the evaporator temperature would have been higher, evaporation would have been more pronounced leading to a higher p_{v_max}. This ensures the deeper penetration of meniscus into the condenser section (or more x_{max}) at the same p_r. Thus it becomes possible to reject the absorbed heat (which is also more now due to higher T_e) by sufficiently enough condensation happening due to higher average area available for the same (condensation happens till $L_e + L_a < x < L_e + L_a + L_c$). Hence, the threshold T_e increases visibly (plot for $T_c = 10$ °C is clearly discriminable from other plots in Fig. 2 (a)) if the T_c value crosses a certain limit. Infact because of the same reasons though weak, the plots for $T_c = -20, -10$ and 0 °C are also in the expected order across a major part of shown coordinate plane as clear from Fig. 2 (b). Here, it is worth noting that existence of instability threshold has been experimentally confirmed by Das et al. [2010]. Oscillations were observed to be prevented by a small decrease in T_e at near instability threshold conditions.

Extremities in the Operational Triad This sub-section covers some of the extremities regarding the parameters of operational triad which lead the oscillations to decay. In broad sense, it gives an idea about different qualitative natures of the decay-facilitating operational triad thus helps to have an insight into the responsible factors. It has already been observed that there is a good interdependence among the minimum/maximum allowable values of the triad elements for oscillation sustainability. Thus it is quite reasonable to discuss extremities regarding two parameters only, such that the third one can be adjusted accordingly for intentional decay of oscillations. So here we are keeping T_e as reference such that while analysing the decay of oscillations w.r.t. p_r and T_c, it is assumed that T_e has taken up a value supporting the decay. Following are the four different combinations of these two parameters analysed w.r.t. oscillation sustainability.

Decay at low T_c and high p_r. High p_r and low T_c makes meniscus to have very small or almost no penetration into the condenser section. Thus, starting with the initial meniscus with some liquid film located inside the evaporator, evaporation happens and vapour pressure rises as shown in Fig. 3. Meniscus is pushed into the adiabatic section up to its end ($x = 0.3\ m$). Then it travels back towards the evaporator section after negligible/no penetration into the condenser section. Till meniscus reaches back evaporator section ($x = 0.2, v < 0$), film evaporation continues and sensible heat transfer occurs at dry evaporator wall. The built-up vapour pressure now allows the meniscus to penetrate very less into the evaporator and leave a small film there as it recedes ($v > 0$). Then the process explained earlier repeats and all this goes on for just a few oscillations. During these few oscillations, there is vapour mass addition to the vapour bubble as well as sensible heat transfer between the evaporator wall and vapour, but no heat rejection anywhere. Thus minimum as well as maximum vapour pressure keeps increasing in every cycle in the beginning. This increment in pressure starts decreasing the meniscus penetration into the evaporator and finally eliminates it out totally. Meniscus starts having its left-most extreme position somewhere within adiabatic section itself (x_{min} increases during each oscillation). So maximum vapour pressure starts decreasing in every oscillation for a few oscillations now, but the minimum vapour pressure still keeps on increasing. This is because of the continued sensible heat transfer at dry section of evaporator. Thus there is heat and mass accumulation at vapour bubble during this initial stage. Thus finally, there is no penetration into either of evaporator and condenser. After few oscillations only within the adiabatic section due to pressure difference and inertia, meniscus finally stops somewhere at adiabatic section ($L_e < x < L_e + L_a$).

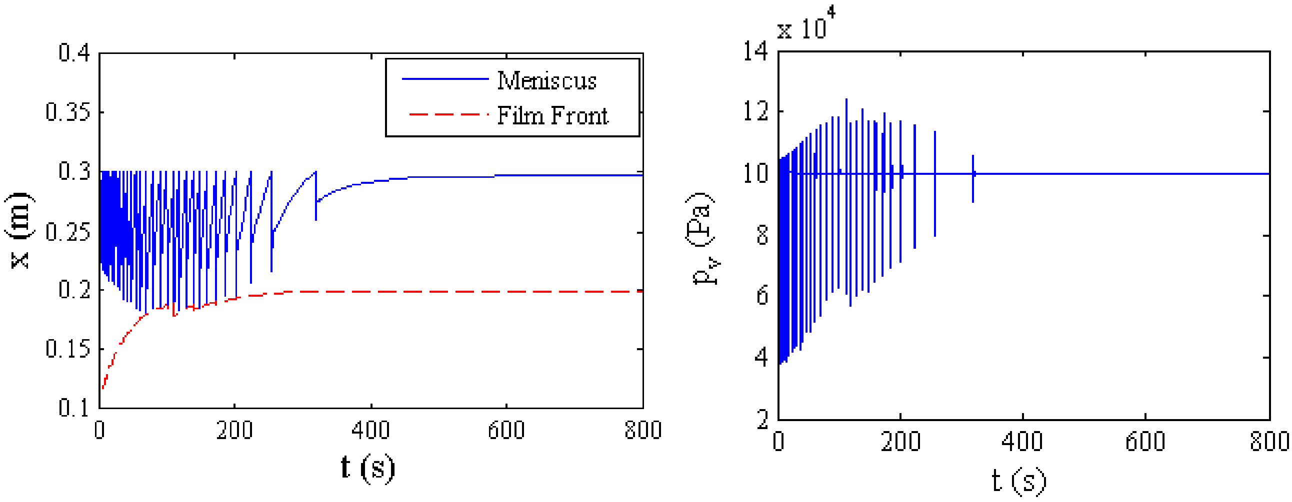

(a) (b)

Fig. 3. Temporal evolution of (a) Meniscus and film front position and (b) Pressure of vapour bubble for $T_e \approx 36$ °C, $T_c = -20$ °C and $p_r = 1$ bar

Thus in short, here we can say that inability of meniscus to enter condenser section lays in the basis of the oscillation decay.

Decay at high T_c and low p_r. As the film evaporates, heat (sensible plus latent) as well as vapour mass is added to the bubble at evaporator, the vapour pressure rises and meniscus moves ($v > 0$). As p_r is low, the meniscus can enter into the condenser easily. As T_c is higher, rejection of absorbed heat needs more condensation area. Meniscus penetrates well into the condenser again owing to a low p_r. It comes to rest ($L_e + L_a < x < L_e + L_a + L_c$) momentarily governed majorly by vapour expansion rather than the condensation as explained earlier, and traverses back towards the adiabatic section as shown in Fig. 4 (a). Having rejected only a fraction of the absorbed heat during the trip through condenser, ongoing evaporation from the film inside evaporator as well as sensible heat transfer between the evaporator wall and vapour, the pressure rise significantly as meniscus moves back ($v < 0$) as clear from Fig. 4 (b). It enters adiabatic section, but could not enter evaporator section due to high vapour pressure and low p_r. Thus no more latent heat absorption and vapour mass addition occurs as very initially deposited film would have got already evaporated. Thus owing to the left-most meniscus's extreme position ($L_e < x < L_e + L_a$) located farther from ($x = 0$), maximum vapour pressure decreases. Now as the vapour pressure (p_{v_max}) is lower, meniscus penetrates lesser into the condenser section, thus again rejects only some part of heat and vapour mass due to condensation. As it moves back it penetrates deeper into adiabatic section but still cannot make it up to evaporator. This way over some cycles, p_{v_max} decreases, penetration into condenser decreases with that in evaporator being always zero (high T_c implies lower pressure drop ($v > 0$) not allowing meniscus to be sucked into evaporator). But sensible heat transfer to vapour from evaporator wall continues and vapour mass decreases. p_{v_min} stays more or less constant. Following this trend, meniscus loses penetration into condenser also after a few oscillations. Thus after having a few oscillations only within the adiabatic section (due to pressure difference and inertia), meniscus finally stops somewhere at $L_e < x < L_e + L_a$. It can be noted from Fig. 4 (c) that in this case if the evaporator section temperature is taken quite high, evaporation will be much more pronounced (higher initial p_{v_max}). Thus the meniscus penetrates deep into the condenser section, crosses it and goes beyond it before reversal during initial few oscillations. Due to higher x_{max} and more condensation, meniscus also enters into evaporator during initial oscillations. The film deposited is small, adds a little mass to the vapour bubble by evaporation while there is considerable condensation owing to more x_{max} even though with high T_c. Finally with decreasing vapour mass, zeroing penetration inside evaporator/condenser and other dynamics resulting due to same reasons as earlier, decay happens. Thus in short, here we can say that inability of meniscus to enter evaporator section lays in the basis of the oscillation decay.

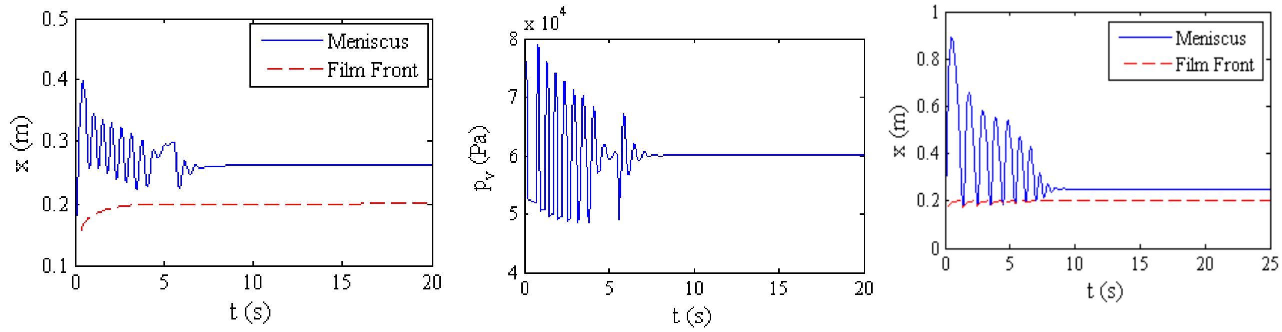

(a) (b) (c)

Fig. 4. Temporal evolution of (a) Meniscus and film front position and (b) Pressure of vapour bubble for $T_e = 30$ °C, $T_c = 16$ °C and $p_r = 0.6$ bar
(c) Meniscus and film front position for $T_e = 60$ °C, $T_c = 16$ °C and $p_r = 0.6$ bar

From the above two cases, it is clear that for T_e supporting the decay, high T_c and high p_r mostly contributes towards ruling out the meniscus penetration into evaporator and condenser respectively. On the contrary, low T_c and low p_r majorly contributes towards ruling out the meniscus penetration into condenser and evaporator sections respectively (only valid again for T_e supporting the decay).

Decay at high T_c and high p_r. Basically the decay happens due to inability of meniscus to enter evaporator as well as condenser, as shown in Fig. 5 (a). It can be noted that pre-decay oscillations are symmetrically localized mainly within the adiabatic section (negligible penetration into evaporator and condenser, leading to small evaporation and condensation respectively). Thus the pre-decay pressure fluctuations are also more or less uniform; p_{v_max} and p_{v_min} are more or less constant for a few oscillations as shown in Fig 5 (b).

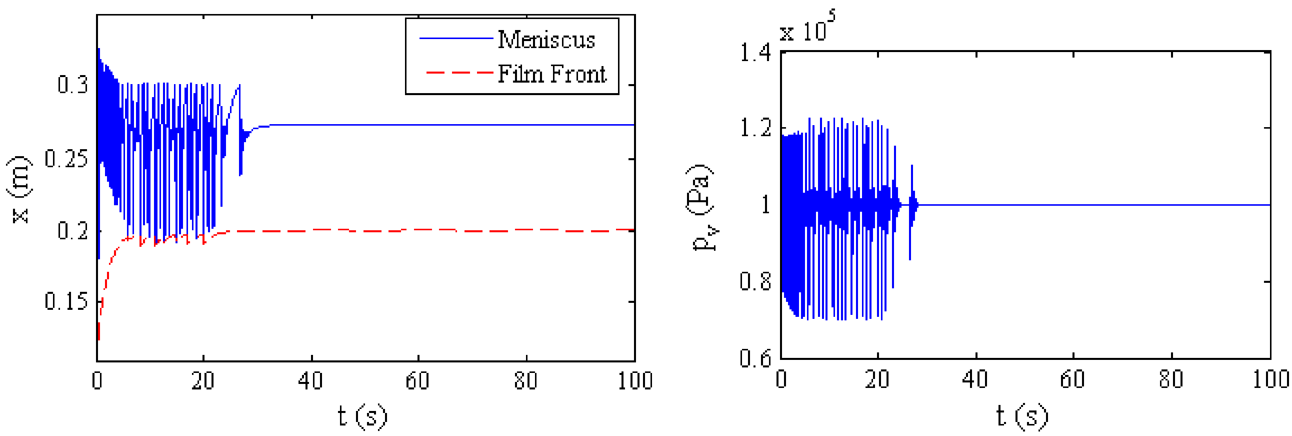

(a) (b)

Fig. 5. Temporal evolution of (a) Meniscus and film front position and (b) Pressure of vapour bubble for $T_e = 40$ °C, $T_c = 25$ °C and $p_r = 1$ bar

Decay at low T_c and low p_r. As explained, decay happens due to inability of meniscus to enter condenser as well as evaporator sections. The decay mechanism would look more or less similar to that shown in Fig. 5.

Decay Mechanism The way the decay of oscillations happens depends upon the factors or parameters which are driving the oscillations to decay. There can be multiple operational or system parameters the combination of which is such that it leads the oscillations to decay. Then the mechanism of decay depends upon all such parameters. Among the driving parameters, one may be the majorly governing parameter, influencing the most the mechanism of decay. The mechanism includes the simultaneous or sequential elimination of meniscus penetration into evaporator/condenser; film deposition, evaporation and complete dry out inside evaporator section etc. Here in this sub-section, the dependence of decay mechanism on one important operational parameter "T_c" has been studied.

Decay mechanism: Dependence on condenser section temperature. For studying the decay mechanism, simulations have been performed with different but high T_c values at $T_e = 50$ °C and $p_r = 0.9$ bar. The corresponding meniscus displacement plots have been shown in Fig. 6 (a) to (d). As already discussed, high T_c value gradually rules out the meniscus penetration into evaporator section which ultimately forms the basis for decay. But this process of ruling out the penetration depends upon the actual T_c value. If the T_c is at the lower limit of the decay-facilitation range of T_c values (Fig. 6 (a)), the meniscus keeps entering into condenser (max 5 cm here) as well as evaporator section (maximum around 1 cm here) for some time. The oscillations are irregular. But it is to be noted from Fig. 6 (a) that meniscus penetrates into evaporator only in alternate oscillations. It has been observed by Das et al. [2010] too for near instability threshold conditions. When it penetrates, it deposits a small film there which then evaporates with the receding motion of meniscus ($v > 0$). But as T_c is quite high leading to very weak condensation, and liquid film evaporation as well as sensible heat transfer to vapour is persistent during this oscillation, the vapour pressure reaches quite high as meniscus comes back towards evaporator again ($v < 0$). As meniscus is unable to enter into evaporator, it exercises a second stroke across the PHP, reducing the vapour mass through condensation (note that there is no evaporation in this stroke as no film is there inside evaporator section). Now with a reduced pressure of vapour bubble (back stroke: $v < 0$), meniscus enters into the evaporator section too. It leaves a small film while receding and the same process goes on for some time. Oscillations persist for some time but with very weak evaporation and condensation. As soon as there is a little accumulation of heat in the vapour bubble though gradual as explained earlier, oscillations come to a stop.

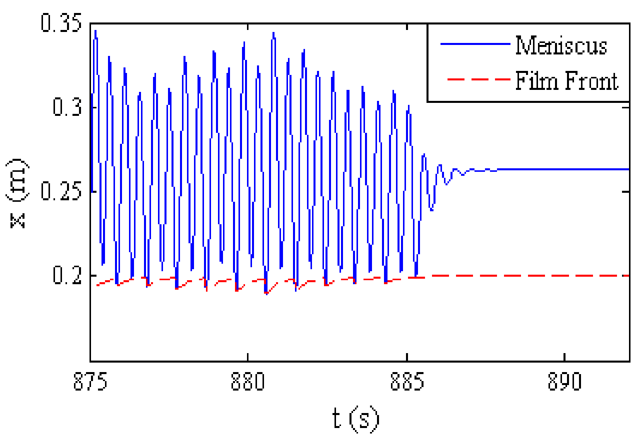

(a) $T_c = 24$ °C

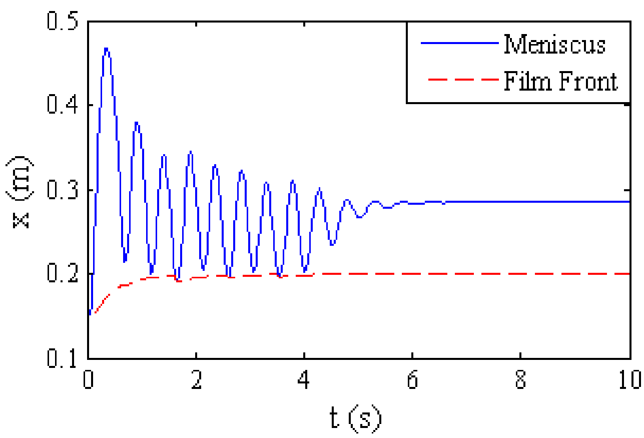

(b) $T_c = 24.2$ °C

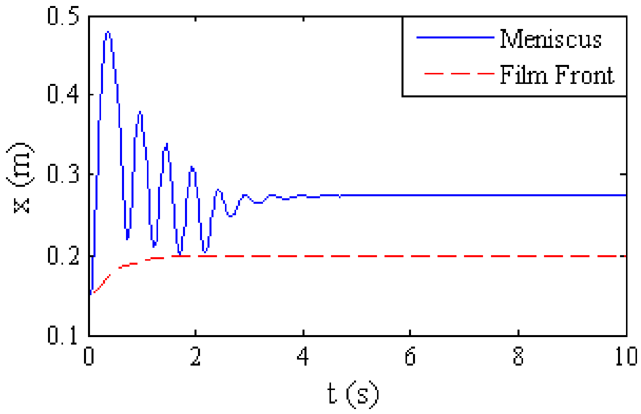

(c) $T_c = 25$ °C

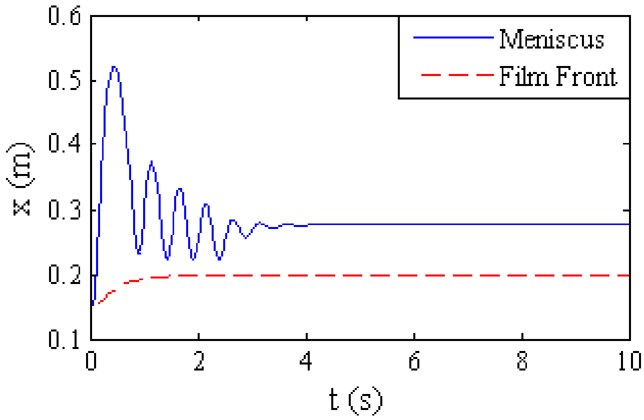

(d) $T_c = 27$ °C

Fig. 6. Temporal evolution of meniscus and film front position for different condenser temperatures at $T_e = 50$ °C and $p_r = 0.9$ bar

As T_c is increased by a small amount over the decay-facilitating lower limit as shown in Fig. 6 (b), meniscus penetrates deeper into condenser section during the first oscillation. But due to the reason explained earlier, it enters into the evaporator section only during the third cycle. But, due to higher T_c resulting into even weaker condensation and higher vapour pressures (when $v < 0$), penetration of the meniscus into evaporator in alternate cycle is almost negligible. It leads to too weak film evaporation and subsequent decay of oscillation.

For the similar reasons, meniscus is hardly able to touch the evaporator section after an initial higher penetration into condenser section, that too after a few oscillations as shown in Fig. 6 (c) for $T_c = 25$ °C. The decay occurs even faster. For $T_c = 27$ °C (Fig. 6 (d)), the meniscus after crossing the condenser in first oscillation does not at all come to the evaporator section's boundary. With the initial film completely evaporated during first oscillation itself and no subsequent evaporation accompanied by the vapour mass reduction due to a few strokes through condenser, oscillations stop quickly. Also, it has been noted that as T_c increases, p_{v_min} increases.

Sustained Oscillations After having studied considerably enough about the decaying oscillations, decay mechanisms and the factors responsible for that, a brief insight can be made into determining what all it takes within the operational triad to sustain the oscillations. It has been found that if T_e is sufficiently high with enough $(T_e - T_c)$ (say with low T_c), reservoir pressure (p_r) can be in wide range for sustained oscillations. Oscillations can be sustained then at significantly low as well as high p_r values. Two cases have been shown in Figures 7 and 8 in this context. It can be noted that for a T_e value facilitating the oscillations to sustain, low p_r facilitates good penetration into evaporator as well as condenser sections. This is because of low p_r allowing the meniscus penetrate very deep into the condenser section (30 cm here, which is up to its right end) coupled with a strong condensation owing to low T_c. Due to significant pressure drop, meniscus is pulled good enough (10 cm here) into the evaporator section as well. Long film deposited there with the receding meniscus ($v > 0$) coupled with high T_e facilitates strong evaporation. Thus everything turns out to be positive and oscillations are sustained. High oscillation amplitude results into smaller frequency as clear from Fig. 7.

With a higher p_r (1 bar here), penetration into both of the evaporator and condenser sections is reduced. Even with the reduced penetration (6 cm here) into condenser section, condensation still happens well owing to a low T_c.

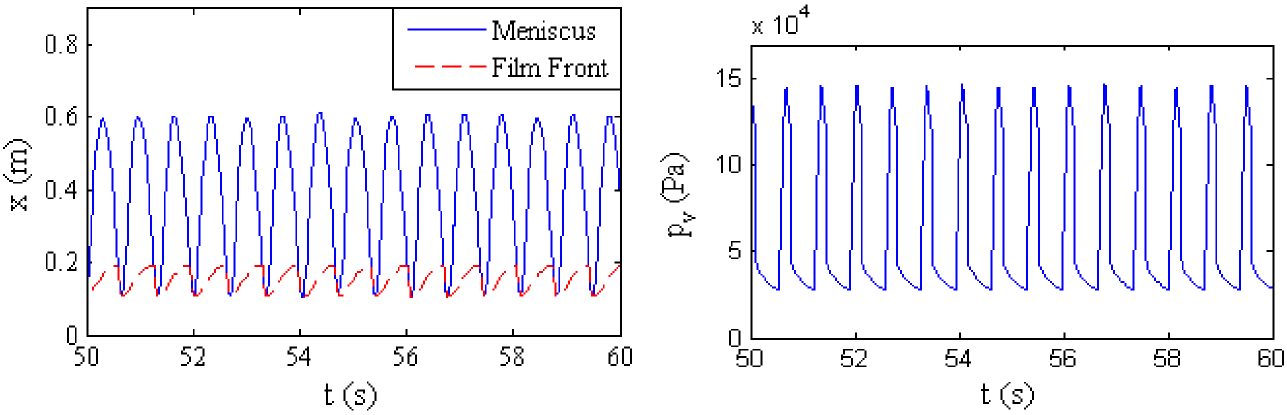

(a) (b)

Fig. 7. Temporal evolution of (a) Meniscus and film front position and (b) Pressure of vapour bubble for $T_e = 50$ °C, $T_c = 0$ °C and $p_r = 0.6$ bar

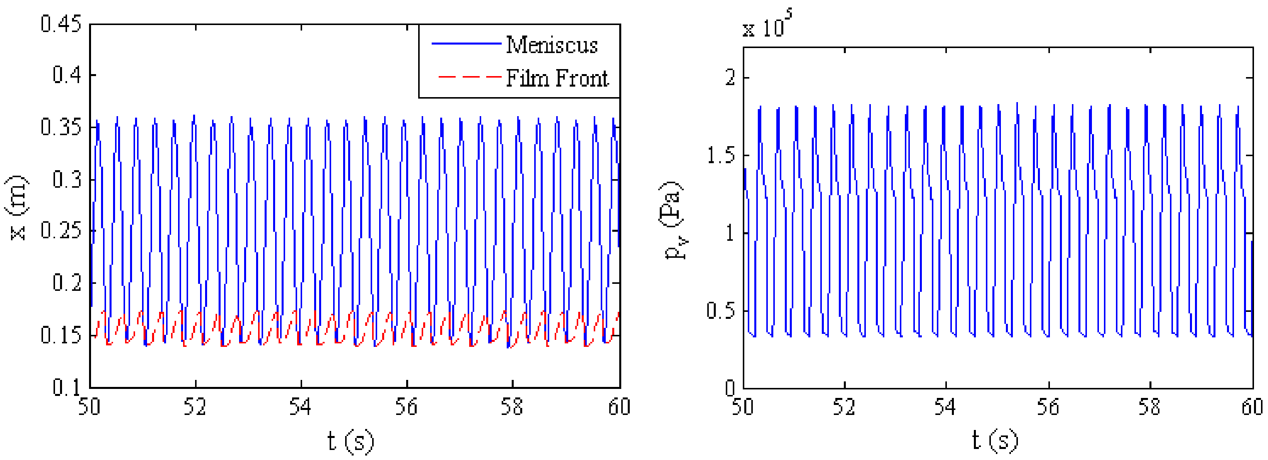

(a) (b)

Fig. 8. Temporal evolution of (a) Meniscus and film front position and (b) Pressure of vapour bubble for $T_e = 50$ °C, $T_c = 0$ °C and $p_r = 1$ bar

With a sufficient pressure drop (though lesser than earlier owing to lesser condensation and vapour expansion), meniscus is pulled into evaporator section (7 cm here, lesser than earlier). Smaller amplitude oscillations proceed with a higher frequency as clear from Fig. 8. It can be noted here that with increase in p_r, p_{v_max} as well as p_{v_min} increases. Here it is worth noting that under such kind of favourable conditions, oscillations have been experimentally observed to be well sustained by Das et al. [2010] too.

CONCLUSIONS

This paper highlights on some of the parameters and factors which play a very important role in deciding whether a single branch pulsating heat pipe is able to sustain its oscillations for long or not. For a specific model geometry incorporating the effects of realistic dynamic frictional losses up to some extent, the governing differential equations based on Film Evaporation/Condensation (FEC) model have been numerically solved. A group of three parameters, viz., evaporator and condenser section temperatures and fluid reservoir pressure has been recognized as operational triad to have a highly significant impact on the sustainability of oscillations. Relative magnitudes of these three parameters play a key role in deciding the sustainability. In this context, evaporator temperature has been found to be more important than the temperature difference of the evaporator and condenser. Higher reservoir pressure needs higher evaporator section temperature for sustained oscillations. Sustainability demands for penetration of meniscus into both of the evaporator and condenser sections. For a decay-facilitating evaporating section temperature, meniscus penetration into evaporator section is not favoured by high condenser section temperature and low reservoir pressure whereas penetration into condenser section is not favoured by low condenser section temperature and high reservoir pressure. Decay mechanisms have also been discussed in details with respect to one operational parameter. On the other hand, for an evaporator section temperature (with a somewhat low condenser temperature) facilitating the oscillation sustainability, high as well as low reservoir pressures can sustain the oscillations quite well. With a thought that ensuring sustainability of oscillations is very important while designing a PHP, a baseline for determining the same has been provided. The study can be extended for multi-branch PHPs and more realistic scenarios.

ACKNOWLEDGEMENTS

Authors are highly thankful to Indian Institute of Technology Madras for its high-end computational facilities which have been used for carrying out simulations at a good pace. Authors are also very grateful to the fellow research scholars at Department of Mechanical Engineering, IIT Madras for helping indispensably in carrying out the post-simulation analysis.

REFERENCES

Akachi, H., Polasek, F. and Stulc, P. (1996). Pulsating Heat Pipes. In: *Proceedings of 5th International Heat Pipe Symposium*. Melbourne: IHPS, pp. 208–217.

Aussilous, P. and Quéré, D. (2000). Quick Deposition of a Fluid on the Wall of a Tube. *Physics of Fluids*, Volume 12, Number 10, pp. 2367–2371.

Bhardwaj, U. and Das, S.P. (2016). Stability and Equilibrium: Dynamics of Adiabatic Section in a Pulsating Heat Pipe. In: *Proceedings of 6th International and 43rd National Conference on Fluid Mechanics and Fluid Power (FMFP)*. Allahabad: FMFP.

Bretherton, F.P. (1961). The Motion of Long Bubbles in Tubes. *Journal of Fluid Mechanics*, Volume 10, Issue 2, pp. 166–188.

Cui, X., Qiu, Z., Weng, J. and Li, Z. (2016). Heat Transfer Performance of Closed Loop Pulsating Heat Pipes with Methanol-based Binary Mixtures. *Experimental Thermal and Fluid Science*, Volume 76, pp. 253–263.

Das, S.P., Nikolayev, V.S., Lefevre, F., Pottier, B., Khandekar, S. and Bonjour, J. (2010). Thermally Induced Two-phase Oscillating Flow inside a Capillary Tube. *International Journal of Heat and Mass Transfer*, Volume 53, Issues 19-20, pp. 3905-3913.

de Gennes, P.G. (1985). Wetting: Statics and Dynamics. *Reviews of Modern Physics*, Volume 57, No. 3, Part I, pp. 827–863.

Dobson, R.T. (2004). Theoretical and Experimental Modelling of an Open Oscillatory Heat Pipe including Gravity. *International Journal of Thermal Sciences*, 43 (2), pp. 113–119.

Dobson, R.T. (2005). An Open Oscillatory Heat Pipe Water Pump. *Applied Thermal Engineering*, 25(4), pp. 603–621.

Faghri, A. (1995). *Heat Pipe Science and Technology*. Bristol, Pennsylvania: Taylor and Francis.

Fairbrother, F. and Stubbs, A.E. (1935). Studies in Electro-endosmosis. Part VI. The Bubble-tube Method of Measurement. *Journal of Chemical Society*, Issue 0, pp. 527–529.

Goshayeshi, H.R., Safaei, M.R., Goodarzi, M. and Dahari, M. (2016). Particle Size and Type Effects on Heat Transfer Enhancement of Ferro-nanofluids in a Pulsating Heat Pipe. *Powder Technology*, Volume 301, pp. 1218–1226.

Han, Y. and Shikazono, N. (2009). Measurement of the Liquid Film Thickness in Micro Tube Slug Flow. *International Journal of Heat and Fluid Flow*, Volume 30, Issue 5, pp. 842–853.

Jiansheng, W., Zhenchuan, W. and Meijun, L. (2014). Thermal Performance of Pulsating Heat Pipes with Different Heating Patterns. *Applied Thermal Engineering*, Volume 64, Issues 1–2, pp. 209–212.

Jun, S. and Kim, S.J. (2016). Comparison of the Thermal Performances and Flow Characteristics between Closed-loop and Closed-end Micro Pulsating Heat Pipes. *International Journal of Heat and Mass Transfer*, Volume 95, pp. 890–901.

Kearney, D.J., Suleman, O., Griffin, J. and Mavrakis, G. (2016). Thermal Performance of a PCB Embedded Pulsating Heat Pipe for Power Electronics Applications. *Applied Thermal Engineering*, Volume 98, pp. 798–809.

Nikolayev, V.S. (2013). Oscillatory Instability of the Gas–liquid Meniscus in a Capillary under the Imposed Temperature Difference. *International Journal of Heat and Mass Transfer*, Volume 64, pp. 313-321.

NIST Chemistry Webbook, NIST Standard Reference Database 69. < http://webbook.nist.gov>.

Rao, M., Lefèvre, F., Khandekar, S. and Bonjour, J. (2013). Understanding Transport Mechanism of a Self-sustained Thermally Driven Oscillating Two-phase System in a Capillary Tube. *International Journal of Heat and Mass Transfer*, Volume 65, pp. 451-459.

Rao, M., Lefèvre, F., Khandekar, S. and Bonjour, J. (2015). Heat and Mass Transfer Mechanisms of a Self-sustained Thermally Driven Oscillating Liquid–vapour Meniscus. *International Journal of Heat and Mass Transfer*, Volume 86, pp. 519-530.

Shafii, M.B., Faghri, A. and Zhang, Y. (2001). Thermal Modeling of Unlooped and Looped Pulsating Heat Pipes. *Journal of Heat Transfer*, 123 (6), pp. 1159–1172.

Shi, S., Cui, X., Han, H., Weng, J. and Li, Z. (2016). A Study of the Heat Transfer Performance of a Pulsating Heat Pipe with Ethanol-based Mixtures. *Applied Thermal Engineering*, Volume 102, pp. 1219–1227.

Wu, Q., Xu, R., Wang, R. and Li, Y. (2016). Effect of C60 Nanofluid on the Thermal Performance of a Flat-plate Pulsating Heat Pipe. *International Journal of Heat and Mass Transfer*, Volume 100, pp. 892–898.

Zhang, Y. and Faghri, A. (2008). Advances and Unsolved Issues in Pulsating Heat Pipes. *Heat Transfer Engineering*, 29 (1), pp. 20-44.